cmgh
CELLULAR AND MOLECULAR GASTROENTEROLOGY AND HEPATOLOGY

ORIGINAL RESEARCH

Down-regulation of RalGTPase-Activating Protein Promotes Colitis-Associated Cancer via NLRP3 Inflammasome Activation

Tomoya Iida,[1,*] Daisuke Hirayama,[1,*] Naoki Minami,[2] Minoru Matsuura,[2] Kohei Wagatsuma,[1] Kentaro Kawakami,[1] Kanna Nagaishi,[3] Masanori Nojima,[4] Hiroki Ikeuchi,[5,6] Seiichi Hirota,[7] Ryutaro Shirakawa,[8] Hisanori Horiuchi,[8] and Hiroshi Nakase[1]

[1]Department of Gastroenterology and Hepatology, Sapporo Medical University School of Medicine, Sapporo, Japan; [2]Department of Gastroenterology and Hepatology, Kyoto University Graduate School of Medicine, Kyoto, Japan; [3]Second Department of Anatomy, Sapporo Medical University School of Medicine, Sapporo, Japan; [4]Center for Translational Research, The Institute of Medical Science Hospital, The University of Tokyo, Tokyo, Japan; [5]Division of Lower Gastrointestinal, Department of Surgery, [6]Inflammatory Bowel Disease Center, [7]Department of Surgical Pathology, Hyogo College of Medicine, Nishinomiya, Japan; [8]Department of Molecular and Cellular Biology, Institute of Development, Aging and Cancer, Tohoku University, Sendai, Japan

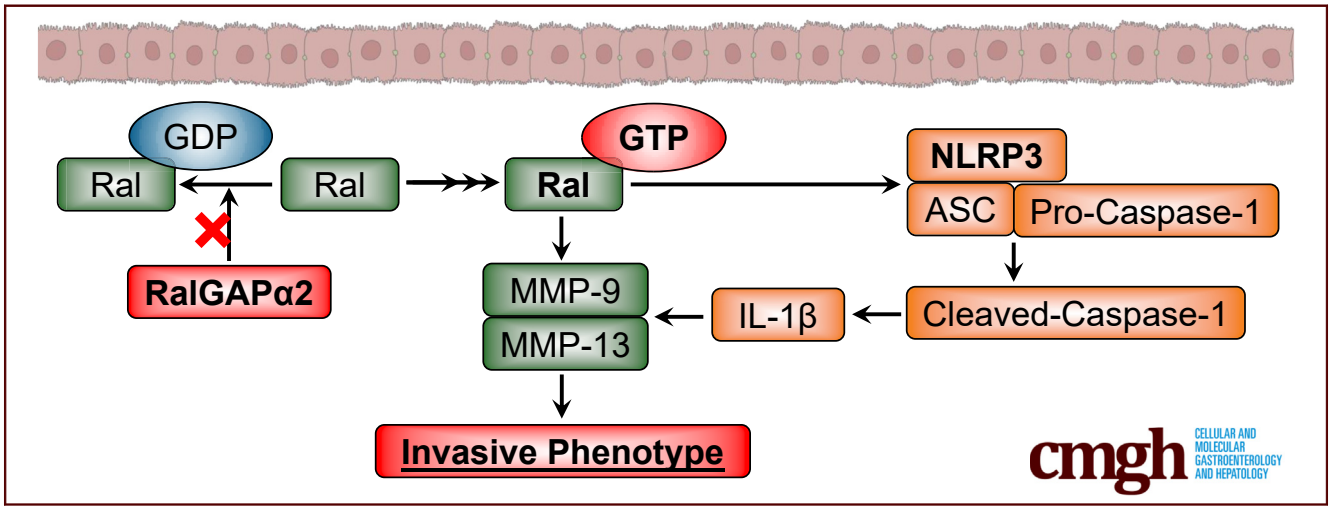

SUMMARY

Ral activation impacts interleukin 1β production by nucleotide-binding domain, leucine-rich–containing family, pyrin domain–containing-3 inflammasome activation and enhances matrix metalloproteinase-9 and matrix metalloproteinase-13 expression in a newly established mouse colitis-associated cancer model. This study strongly showed that the Ras-like-nucleotide-binding domain, leucine-rich–containing family, pyrin domain–containing-3 inflammasome pathway is involved in the mechanism of colitis-associated cancer invasion.

BACKGROUND & AIMS: Ral guanosine triphosphatase–activating protein α2 (RalGAPα2) is the major catalytic subunit of the negative regulators of the small guanosine triphosphatase Ral, a member of the Ras subfamily. Ral regulates tumorigenesis and invasion/metastasis of some cancers; however, the role of Ral in colitis-associated cancer (CAC) has not been investigated. We aimed to elucidate the role of Ral in the mechanism of CAC.

METHODS: We used wild-type (WT) mice and RalGAPα2 knockout (KO) mice that showed Ral activation, and bone marrow chimeric mice were generated as follows: WT to WT, WT to RalGAPα2 KO, RalGAPα2 KO to WT, and RalGAPα2 KO to RalGAPα2 KO mice. CAC was induced in these mice by intraperitoneal injection of azoxymethane followed by dextran sulfate sodium intake. Intestinal epithelial cells were isolated from colon tissues, and we performed complementary DNA microarray analysis. Cytokine expression in normal colon tissues and CAC was analyzed by quantitative polymerase chain reaction.

RESULTS: Bone marrow chimeric mice showed that immune cell function between WT mice and RalGAPα2 KO mice was not significantly different in the CAC mechanism. RalGAPα2 KO mice had a significantly larger tumor number and size and a significantly higher proportion of tumors invading the submucosa than WT mice. Higher expression levels of matrix metalloproteinase-9 and matrix metalloproteinase-13 were observed in RalGAPα2 KO mice than in WT mice. The expression levels of interleukin 1β, NLRP3, apoptosis associated speck-like protein containing a CARD, and caspase-1 were apparently increased in the tumors of RalGAPα2 KO mice compared with WT mice. NLRP3 inhibitor reduced the number of invasive tumors.

CONCLUSIONS: Ral activation participates in the mechanism of CAC development via NLRP3 inflammasome activation. *(Cell*

Mol Gastroenterol Hepatol 2020;9:277–293; https://doi.org/10.1016/j.jcmgh.2019.10.003)

Keywords: Ral; Ral-GTPase Activating Protein (RalGAP); Colitis-Associated Cancer; NLRP3 Inflammasome.

Patients with long-standing inflammatory bowel disease (IBD) are at high risk for developing dysplasia and colitis-associated cancer (CAC). In clinical practice, detecting dysplasia and CAC at endoscopy often is difficult. In addition, CAC has a tendency to easily invade intestinal tissues.[1] Therefore, these clinicopathologic features result in the poor prognosis of IBD patients with CACs. Several studies have indicated that sustained intestinal inflammation plays a substantial role in increasing CAC via telomere shortening, DNA damage, and cellular senescence.[2] However, the exact molecular mechanism of CAC remains unclear.

The small guanosine triphosphatase (GTPase) Ras-like (Ral), a member of the Ras subfamily, is known to control various cellular functions by mediating multiple effector molecules,[3,4] and Ral plays an important role in cell survival by acting through the regulation of TRAF (tumor necrosis factor receptor-associated factor) family member associated NF-KB (nuclear factor-kappa B) activator (TANK)-binding kinase 1, which is the controlling factor of nuclear factor-κB (NF-κB).[5] Thus, Ral also is involved in inflammation. Ral has 2 isoforms: RalA and RalB. RalA and RalB have been shown to play different roles in human cancer: RalA is involved in anchorage-independent growth, and RalB is required for cell survival and migration.[6–8]

Ral is positively regulated by Ral guanine nucleotide exchange factors, several of which are effector molecules of Ras. Thus, Ral is activated downstream of active Ras. However, Ral is inactivated by RalGTPase-activating proteins (RalGAPs) that we identified previously.[9] RalGAPs are heterodimers of a common β subunit and a catalytic α subunit (RalGAPα1 or RalGAPα2). The heterodimer comprising RalGAPα1 and the RalGAP β subunit is designated RalGAP1, and the heterodimer comprising RalGAPα2 and the RalGAP β subunit is designated RalGAP2.[10] Complex formation is essential for RalGAP activity and protein stability, and loss of either subunit leads to the inactivation of its enzyme activity. Each form of RalGAP regulates both RalA and RalB.[9]

The expression of the α subunit varies among different organ types. We previously reported that RalGAPα2 knockout (KO) mice developed muscle-invasive bladder cancers that were not found in wild-type (WT) mice in chemically induced bladder carcinogenesis models.[11] In addition, we reported that loss of RalGAPα2 promoted local microscopic invasion of prostatic intraepithelial neoplasia in a phosphatase and tensin homolog deleted from chromosome 10–deficient mouse model for prostate tumorigenesis in a recent study.[12] In addition, Kodama et al[13] reported a significant reduction in RalGAPα2 expression in hepatocellular carcinoma and a role for RalGAPα2 in the enlargement of hepatocellular carcinoma. These data suggest that RalGAPα2 plays an important role in the development or invasion mechanism in some cancers. However, the precise role of RalGAPα2 in CAC has not been elucidated.

In the present study, we show that RalGAPα2 is highly expressed in the normal colon epithelium and in sporadic colorectal cancer compared with CAC in human samples. In addition, Ral activation greatly enhances tumor invasion, with matrix metalloproteinase (MMP)-9 and MMP-13 expression. Furthermore, Ral activation impacts interleukin (IL)1β production by NLRP3 inflammasome activation. Our data strongly show that the Ral-NLRP3 inflammasome pathway is involved in the mechanism of CAC invasion.

Results

RalGAPα2 Is Expressed Mainly in Colon Epithelial Cells but Not in Immune Cells

Western blot (WB) analysis showed that mouse colon tissues strongly expressed the RalGAPα2 subunit but showed little expression of RalGAPα1 (Figure 1*A*). In addition, both the human and mouse colon cancer cell lines strongly expressed the RalGAPα2 subunit but showed little expression of RalGAPα1 (Figure 1*B*). Furthermore, WB analysis showed that the expression levels of both RalGAPα1 and α2 were weak in monocytes, T cells, and B cells (Figure 1*B*).

Knockdown (KD) of RalGAPα2 (Figure 1*C*) increased the activation of RalA and RalB (Figure 1*D* and *F*), and slightly increased the expression levels of total RalA and total RalB (Figure 1*E* and *G*) in Colon26 cells. The RalA-GTP/total-RalA and RalB-GTP/total-RalB ratios were significantly higher in the RalGAPα2 KD Colon26 cells than in the controls (Figure 1*H*).

RalGAP Does Not Influence T-Helper Cell 1/2/17 or B-Cell Differentiation or Cytokine Production in Macrophages

Under the steady-state condition, flow cytometry analysis showed no significant difference in T-helper cell (Th)1/Th2/Th17 differentiation of CD4-positive T cells and B-cell differentiation of CD19-positive B cells between WT mice and RalGAPα2 KO mice (Figure 2*A* and *B*). In addition, no

***Authors share co-first authorship.**

Abbreviations used in this paper: **AOM, azoxymethane; ASC, apoptosis associated speck-like protein containing a CARD; CAC, colitis-associated cancer; DSS, dextran sulfate sodium; GTPase, guanosine triphosphatase; IBD, inflammatory bowel disease; IL, interleukin; KD, knockdown; KO, knockout; KO-N, normal colon tissues of RalGAPα2 knockout mice; KO-T, tumors of RalGAPα2 knockout mice; MMP, matrix metalloproteinase; mRNA, messenger RNA; NF-κB, nuclear factor-κB; qPCR, quantitative polymerase chain reaction; RalGAP, Ral guanosine triphosphatase–activating protein; siRNA, small interfering RNA; SM, submucosal; STAT3, signal transducer and activator of transcription 3; Th, T-helper cell; TNF-α, tumor necrosis factor α; WB, Western blot; WT, wild-type; WT-N, normal colon tissues of wild-type mice; WT-T, tumors of wild-type mice.**

Most current article

2352-345X
https://doi.org/10.1016/j.jcmgh.2019.10.003

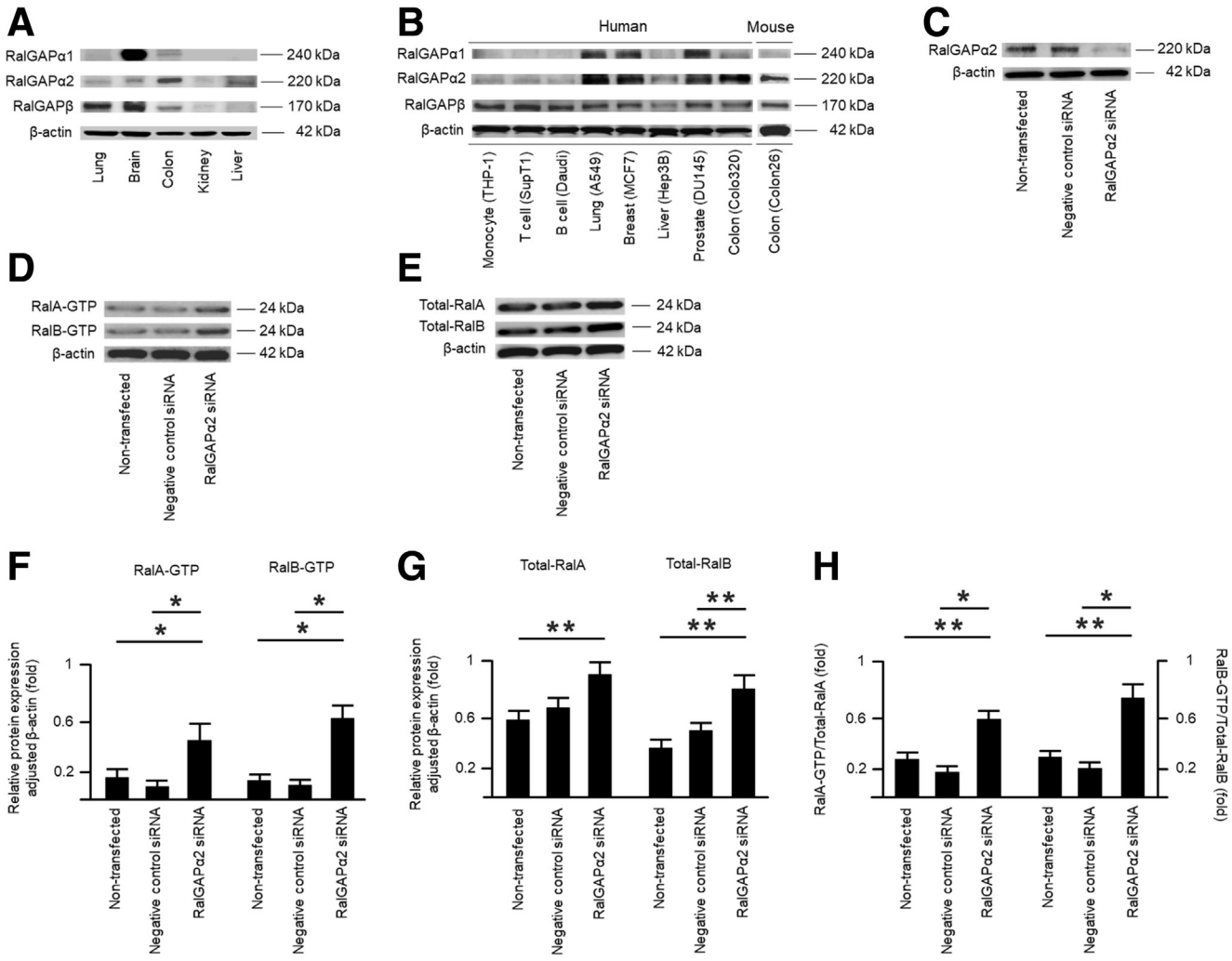

Figure 1. (*A* and *B*) The difference in RalGAP expression was analyzed by Western blot. (*C*) RalGAPα2 knockdown was evaluated by Western blot. (*D* and *E*) The differences in the expression levels of RalA, RalB, total RalA, and total RalB in controls and RalGAPα2 knockdown Colon26 cells were analyzed by Western blot. (*F* and *G*) Densitometric analysis of the expression levels of RalA-GTP, RalB-GTP, total RalA, and total RalB in controls and RalGAPα2 knockdown Colon26 cells by Western blot. *$P < .01$, **$P < .05$, repeated-measures analysis of variance with the Holm correction. (*H*) The ratios of the expression of RalA-GTP/total RalA and RalB-GTP/total RalB in the RalGAPα2 knockdown Colon26 cells. *$P < .01$, **$P < .05$, repeated-measures analysis of variance with the Holm correction. Data are either representative or shown as the means ± SEM (error bars) of 3 independent experiments.

significant differences were observed in the cytokines (IL1β, IL12A, or tumor necrosis factor-α [TNF-α]) released from intraperitoneal macrophages collected after intraperitoneal administration of thioglycolate between the WT mice and RalGAPα2 KO mice (Figure 2*C*). These results did not change under the dextran sulfate sodium (DSS) condition (Figure 2*D*–*F*). These findings showed that RalGAP did not influence T-cell or B-cell differentiation or cytokine production of macrophages regardless of the administration of DSS.

RalGAPα2 Expression Is Decreased in CAC

We compared the expression levels of RalGAPα2 in human normal colon tissue, sporadic colorectal cancer, and CAC samples by immunohistochemical staining (Figure 3*A*). The ratios showing strong RalGAPα2 staining in the normal colon tissue, sporadic colorectal cancer, and CAC samples were 85.7% (30 of 35), 80.0% (12 of 15), and 25% (5 of 20), respectively. Thus, the expression of RalGAPα2 in CAC was significantly lower than that in normal colon tissue or sporadic colorectal cancer (Figure 3*B*). When CAC is divided into 2 groups as noninvasive and invasive, the ratios showing strong RalGAPα2 staining in noninvasive and invasive CAC samples were 80.0% (4 of 5) and 6.7% (1 of 15), respectively (Figure 3*C*). Therefore, the expression of RalGAPα2 decreased, that is, activation of Ral was observed at a more advanced stage in CAC. In addition, patient information from the human cohort is shown in Figure 3*D*. There were no significant differences in patients' backgrounds between patients with sporadic colorectal cancer and those with CAC.

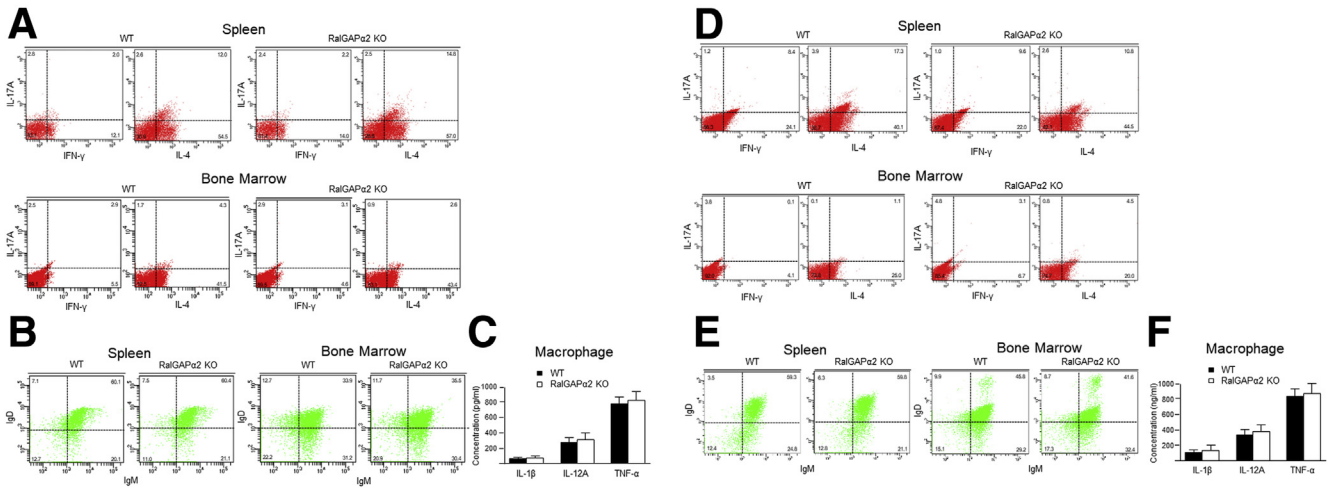

Figure 2. (*A–C*) The differences in the contributions of immune cells in steady state between WT mice and RalGAPα2 KO mice were analyzed by flow cytometry or enzyme-linked immunosorbent assay. (*A*) T-cell differentiation. (*B*) B-cell differentiation. (*C*) Cytokine expression of macrophages (1-way analysis of variance with the Holm correction). (*D–F*) The differences in the contributions of the immune cells after dextran sulfate sodium treatment between WT mice and RalGAPα2 KO mice were analyzed by flow cytometry or enzyme-linked immunosorbent assay. (*D*) T-cell differentiation. (*E*) B-cell differentiation. (*F*) Cytokine expression of macrophages (1-way analysis of variance with the Holm correction). Data are either representative or shown as means ± SEM (error bars) of 3 independent experiments. IFN, interferon.

RalGAPα2 KO Mice Treated With Azoxymethane/DSS Develop Invasive Tumors

The azoxymethane (AOM)/DSS administration protocol is shown in Figure 4*A*. Tumor occurrence was examined at the distal end of the colon tissue by endoscopy (Figure 4*B*), macroscopic images (Figure 4*C*), and histopathologic findings (Figure 4*D*). The RalGAPα2 KO mice developed more tumor growth in terms of number (WT vs RalGAPα2 KO, 4.5 ± 2.3 vs 7.6 ± 2.4) (Figure 4*E*) and larger tumor sizes (WT vs RalGAPα2 KO, 3.3 ± 1.6 vs 5.7 ± 2.0 mm) (Figure 4*F*) than the WT mice. The ratio of mice having submucosal (SM) invasive tumors in the RalGAPα2 KO group was higher than that in the WT group (WT vs RalGAPα2 KO, 5.0% [1 of 20] vs 45.0% [9 of 20]) (Figure 4*G*). In addition, the number of SM invasive tumors in the cancer specimens from the RalGAPα2 KO mice was higher than that in the specimens from the WT mice (WT vs RalGAPα2 KO, 2.9% [2 of 70] vs 20.0% [24 of 120]) (Figure 4*H*). Taken together, these observations strongly indicate that Ral activation promoted tumor development or CAC progression.

Next, we examined Ral activation in mouse colon tissues. The pull-down analysis showed that the tissues from the RalGAPα2 KO mice (normal colon tissues of RalGAPα2 KO mice [KO-N] and tumors of RalGAPα2 KO mice [KO-T]) showed increased activation of RalA and RalB (Figure 4*I* and *K*) and slightly increased expression levels of total RalA and total RalB (Figure 4*J* and *L*). The RalA-GTP/total-RalA and RalB-GTP/total-RalB ratios in the tissues from the RalGAPα2 KO mice were significantly higher than those in the tissues from the WT mice. These ratios were increased markedly in the KO-T mice (Figure 4*M*). These findings suggest that the down-regulation of RalGAPα2 induced Ral activation, especially in colon tumors.

Bone Marrow Chimeric Mice Showed RalGAPα2 Did Not Affect Immune Cell Function

To confirm the contribution of RalGAPα2 in immune cells to CAC in vivo, we generated bone marrow chimeric mice and divided them into 4 groups, as follows: (1) WT to WT, (2) WT to RalGAPα2 KO, (3) RalGAPα2 KO to WT, and (4) RalGAPα2 KO to RalGAPα2 KO mice, and CAC was induced in these mice by the AOM/DSS protocol shown in Figure 5*A*. Tumor occurrence was examined at the distal end of the colon tissues by macroscopic images (Figure 5*B*) and histopathologic findings (Figure 5*C*). Compared with the totally WT mice (group 1), the totally RalGAPα2 KO mice (group 4) developed significantly more tumor growth in terms of number (group 1 vs group 4, 3.6 ± 1.6 vs 6.1 ± 2.1) (Figure 5*D*) and larger tumor sizes (group 1 vs group 4, 2.9 ± 1.4 vs 7.4 ± 2.6 mm) (Figure 5*E*). Although it was not significant ($P = .07$), the ratio of mice with SM invasive tumors in group 4 was higher than that in group 1 (group 1 vs group 4, 0% [0 of 10] vs 37.5% [3 of 8]) (Figure 5*F*). In addition, the number of SM invasive tumors in the cancer specimens in group 4 was significantly higher than that in the specimens in group 1 (group 1 vs group 4, 0% [0 of 20] vs 28.6% [8 of 28]) (Figure 5*G*). These results were consistent with the results in the mouse CAC model described earlier (Figure 4*A–H*).

In addition, there were no differences between group 1 and group 2, or between group 3 and group 4, in the number of tumors (Figure 5*D*), the tumor maximum diameter (Figure 5*E*), the ratio of mice with SM invasive tumors (Figure 5*F*), and the number of SM invasive tumors in the cancer specimens (Figure 5*G*). Taken together, these observations strongly indicate that RalGAPα2 did not affect immune cell function in the mouse CAC model.

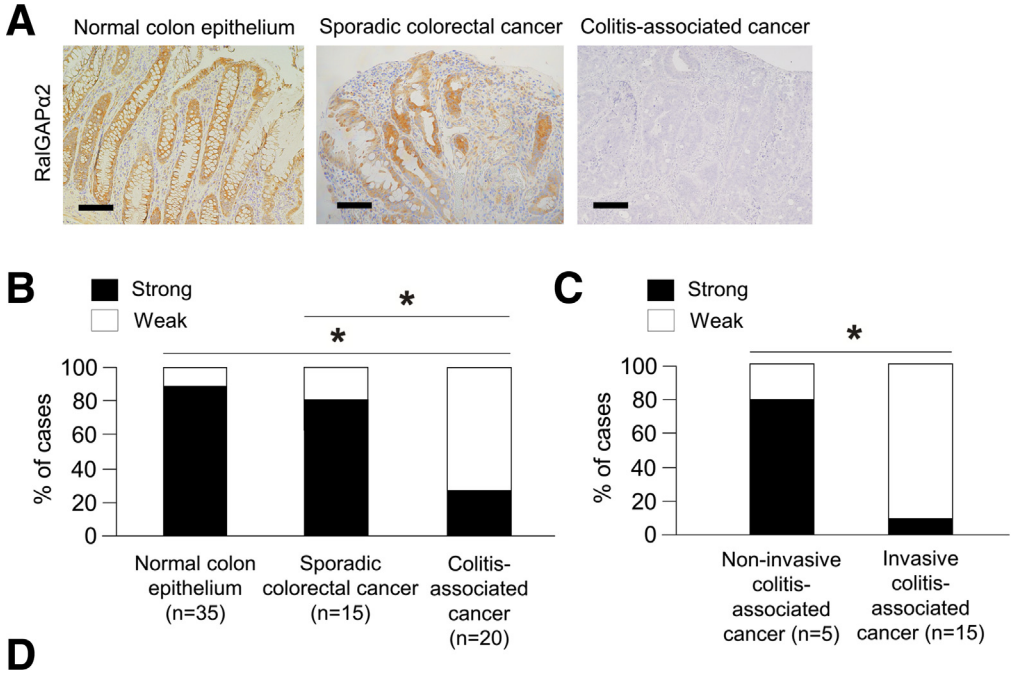

Figure 3. (*A*) **Immunohistochemical staining of RalGAPα2 on part of the normal colon epithelium, sporadic colorectal cancer, and CAC (original magnification, 100×).** *Scale bars*: 100 μm. Data are representative of each tissue. (*B*) Strong staining rate of RalGAPα2 using human colon tissues (normal colon epithelium, n = 35; sporadic colorectal cancer, n = 15; and CAC, n = 20). *$P < .01$, Fisher exact test with the Holm correction. (*C*) Strong staining rate of RalGAPα2 using human CAC tissues (noninvasive CAC, n = 5; and invasive CAC, n = 15). *$P < .01$, Fisher exact test. (*D*) Patient information on the human cohort (sporadic colorectal cancer, n = 15; and CAC, n = 20) (Student *t* test, Fisher exact test). CD, Crohn's disease; N/A, not applicable; UC, ulcerative colitis; UICC, Union for International Cancer Control.

D

	Sporadic colorectal cancer (n=15)	Colitis-associated cancer (n=20)	*P* value
Average age (±SD) (years)	64 (±16.9)	52 (±13.1)	.24
Sex (Male: Female)	5: 10	10: 10	.49
Underlying disease (UC: CD)	N/A	20: 0	N/A
Colitis range (Left: Total)	N/A	5: 15	N/A
Average disease duration (±SD) (years)	N/A	21.9 (±7.7)	N/A
TNM classification (UICC 8th edition)			
T (is-1: 2-4)	6: 9	5: 15	.47
N (0: 1-2)	10: 5	13: 7	1.0
M (0: 1)	12: 3	19: 1	0.29
Stage (I-II: III-IV)	10: 5	13: 7	1.0

RalGAPα2 KD Colon26 Cells Show Increased Migratory and Invasive Capacities

The in vitro wound healing (Figure 6*A*) and cell invasion assays (Figure 6*B*) showed that significantly more RalGAPα2 KD Colon26 cells than control cells migrated and invaded. In addition, Ral activation correlated with an increase in the cell migratory and invasive capacities.

MMP-9 and MMP-13 Expression Levels Are Up-Regulated in Colon Tumors From RalGAPα2 KO Mice

Phenotypic differences in colonic epithelial cells from both WT mice and RalGAPα2 KO mice were examined. Colonic epithelial cells were isolated from colon tissues, and flow cytometry was performed to determine whether more than 90% of the isolated cells were CD326-positive/CD45-negative epithelial cells (Figure 6*C*). Then, microarray analysis showed that the gene expression levels of *MMP-9* and *MMP-13* in colon epithelial cells from the RalGAPα2 KO mice increased to more than twice those of the WT mice. On the other hand, the *MMP-2*, *-3*, *-7*, and *-12* gene expression levels in the RalGAPα2 KO mice did not increase compared with those in the WT mice (Figure 6*D*).

Quantitative polymerase chain reaction (qPCR) showed that MMP-9 and MMP-13 messenger RNA (mRNA) expression in the KO-T significantly increased compared with that in the tumors of WT mice (WT-T) (Figure 6*E*). Gelatin zymography analysis showed that activated MMP-9 was increased drastically in the KO-T (Figure 6*F*). WB analysis showed that MMP-13 expression apparently increased in the KO-T (Figure 6*G*). In addition, immunohistochemical staining showed an increased number of cells that were positive for MMP-9 (Figure 6*H*) and MMP-13 (Figure 6*I*) at the invasive fronts of the tumors in the RalGAPα2 KO group compared with the WT group. These results suggest that MMP-9 and MMP-13 are involved in colon tumor invasion in RalGAPα2 KO mice.

IL1β Expression Is Up-Regulated Significantly in Colon Tumors From RalGAPα2 KO Mice

Next, we examined cytokine levels in mouse tissues by qPCR. *IL1β* expression in KO-N was significantly

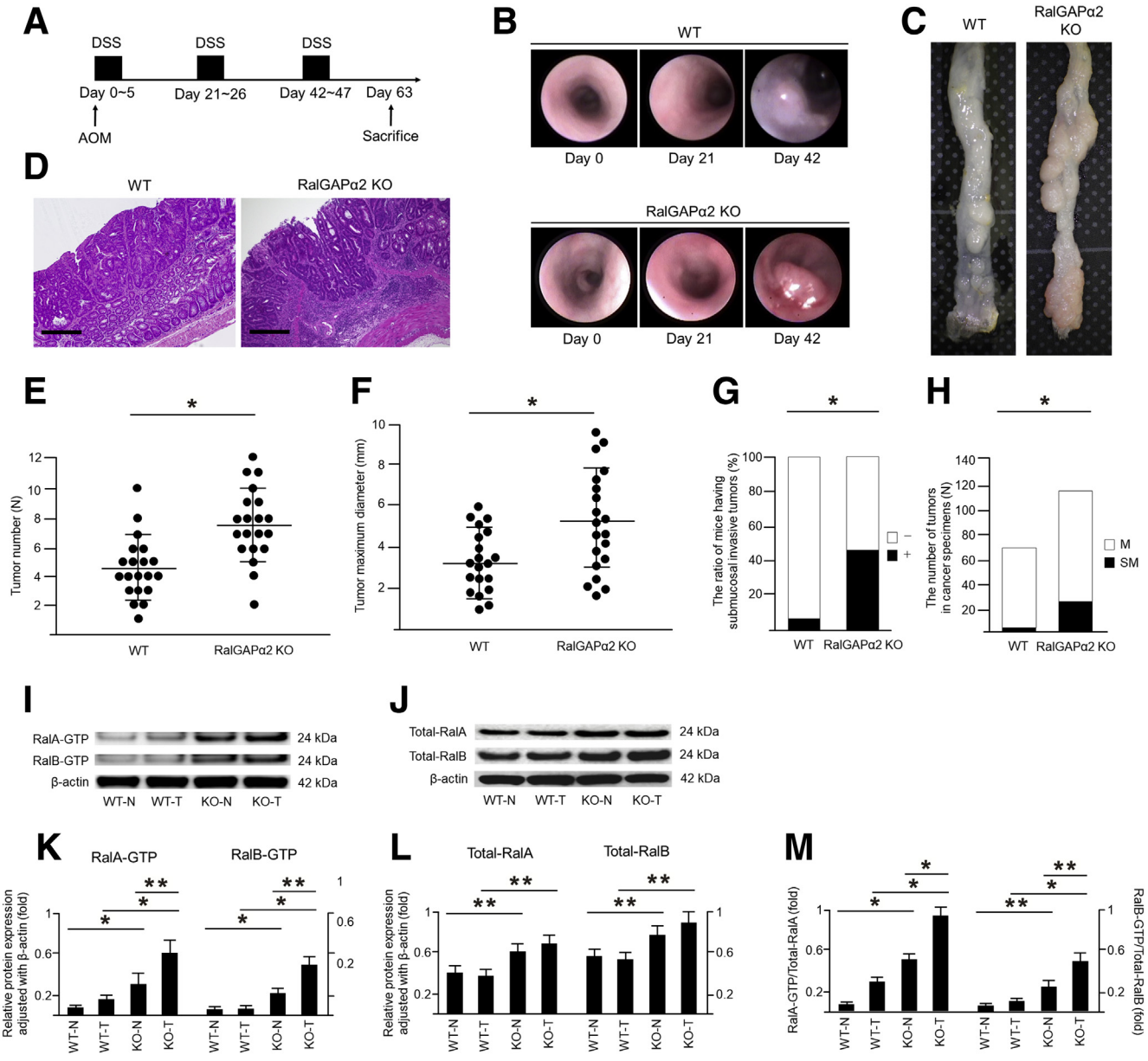

Figure 4. (*A*) The AOM/DSS administration protocol. We performed this protocol in both WT mice (n = 20) and RalGAPα2 KO mice (n = 20). (*B*) The endoscopic findings of colon tumors in WT mice and RalGAPα2 KO mice. (*C*) The macroscopic findings of colon tumors in WT mice and RalGAPα2 KO mice. (*D*) H&E staining of colon sections of WT mice and RalGAPα2 KO mice on day 63 (original magnification, 100×). *Scale bars*: 100 μm. (*E*) Tumor number in the WT mice and RalGAPα2 KO mice. *$P < .01$, Student *t* test. (*F*) Tumor maximum diameter in the WT mice and RalGAPα2 KO mice. *$P < .01$, Student *t* test. (*G*) The ratio of mice with submucosal invasive tumors in the WT mice and RalGAPα2 KO groups. *$P < .01$, Fisher exact test. (*H*) The number of submucosal invasive tumors in the cancer specimens of WT mice and RalGAPα2 KO mice. *$P < .01$, Fisher exact test. (*I* and *J*) The expression of RalA-GTP, RalB-GTP, total RalA, and total RalB in the colonic mucosa and CAC of both WT mice and RalGAPα2 KO mice was analyzed by the glutathione-S-transferase–Sec5 pull-down assay. (*K* and *L*) Densitometric analysis of the expression levels of RalA-GTP, RalB-GTP, total RalA, and total RalB in the colonic mucosa and CAC of both WT mice and RalGAPα2 KO mice by Western blot. (*M*) The ratios of the expression of RalA-GTP/total RalA and RalB-GTP/total RalB in the colonic mucosa and CAC of both WT mice and RalGAPα2 KO mice. Data are either representative or shown as the means ± SEM (error bars) of 3 independent experiments. (*K–M*) *$P < .01$, **$P < .05$ by repeated-measures analysis of variance with the Holm correction.

higher than that in normal colon tissues of WT mice (WT-N). In addition, *IL1β* expression in the KO-T was significantly higher than that in the WT-T or KO-N. The expression levels of *IL4* and *IL13* were significantly lower in the KO-T than in WT-T. There were no differences in the expression levels of *TNF-α, interferon-γ, IL6, IL10, IL12A, IL17,* or *IL18* (Figure 7*A*). These data suggest a strong association between IL1β expression and a CAC-promoting inflammatory environment in RalGAPα2 KO mice.

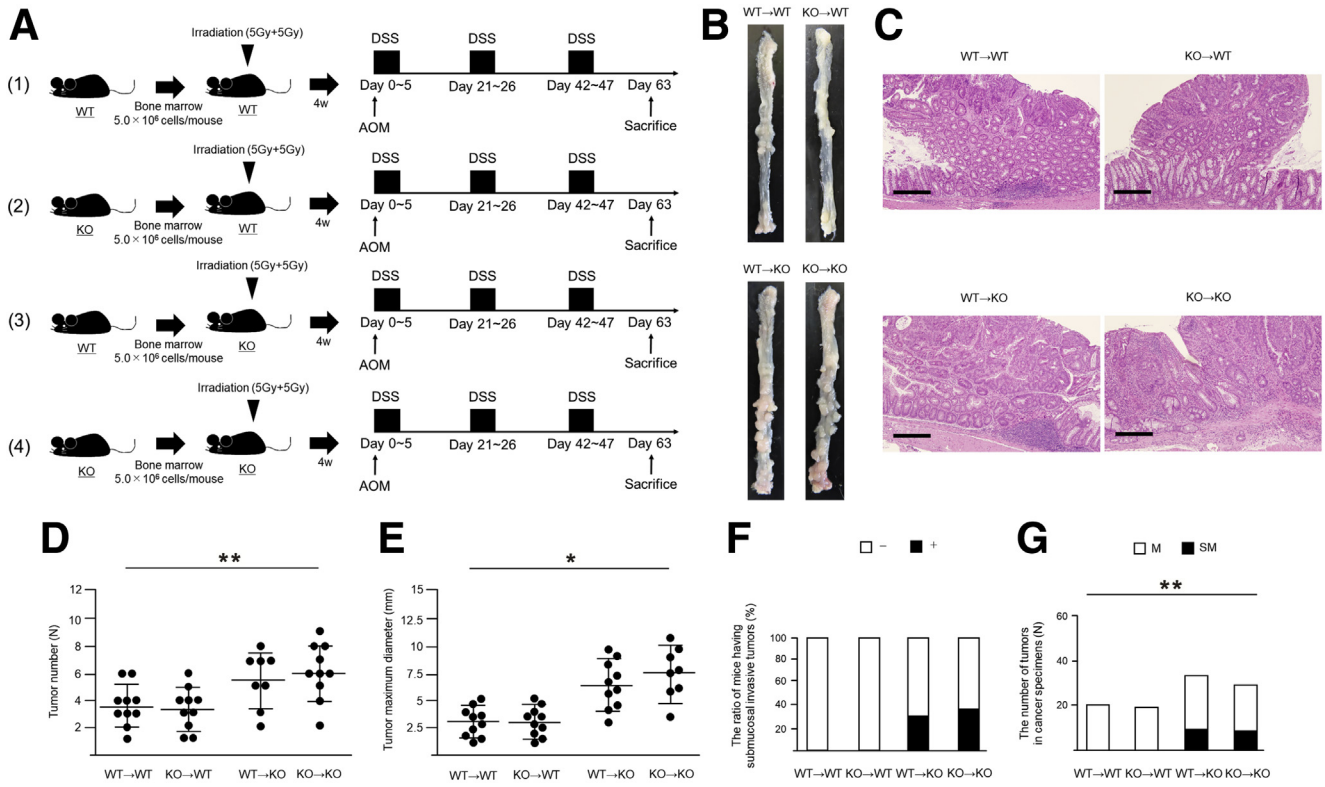

Figure 5. (*A*) Bone marrow chimeric mice were generated as follows: (1) WT to WT (n = 10), (2) WT to RalGAPα2 KO (n = 10), (3) RalGAPα2 KO to WT (n = 10), and (4) RalGAPα2 KO to RalGAPα2 KO mice (n = 8). Four weeks after irradiation (5 Gy + 5 Gy) and bone marrow transfusion (5.0×10^6 cells/mouse), CAC was induced in these mice by intraperitoneal injection of azoxymethane followed by 3 cycles of dextran sulfate sodium intake. (*B*) The macroscopic findings of colon tumors in the chimeric mice. (*C*) H&E staining of colon sections of the chimeric mice on day 63 (original magnification, 100×). *Scale bars*: 100 μm. (*D*) Tumor number in the chimeric mice. $^{**}P < .05$, 1-way analysis of variance with the Holm correction. (*E*) Tumor maximum diameter in the chimeric mice. $^{*}P < .01$, 1-way analysis of variance with the Holm correction. (*F*) The ratio of mice with submucosal invasive tumors in the chimeric mice (Fisher exact test with the Holm correction). (*G*) The number of submucosal invasive tumors in the cancer specimens of the chimeric mice. $^{**}P < .05$, Fisher exact test with the Holm correction.

Down-Regulation of RalGAPα2 Induces Activation of the NLRP3 Inflammasome

Next, we focused on the association between Ral activation and the NLRP3 inflammasome as a main inducer of IL1β. WB analysis showed that RalGAPα2 KD increased the expression levels of NLRP3, apoptosis associated speck-like protein containing a CARD (ASC), pro/cleaved caspase-1, and pro/cleaved caspase-11 in Colon26 cells (Figure 7*B*). In vivo data showed that the expression of NLRP3, ASC, and pro/cleaved caspase-1 tended to be increased in both WT-T and KO-T. These proteins were expressed more strongly in KO-T than in WT-T. Moreover, pro/cleaved caspase-11, NF-κB p65, phosphorylated NF-kappaB p65 (NF-κB p-p65), signal transducer and activator of transcription 3 (STAT3), and phosphorylated STAT3 tended to be increased in KO-N than in WT-N. However, these high expressions were not observed in KO-T (Figure 7*C*). These data indicate that down-regulation of RalGAPα2 did not intensify the noncanonical NLRP3 inflammasome activation or NF-κB–STAT3 signaling, but intensified the canonical NLRP3 inflammasome activation in CAC.

NLRP3 Inhibitor Administration Suppresses the Invasive Potential of Colon26 Cells and of Tumors in RalGAPα2 KO Mice

To evaluate the role of the inflammasome in CAC development in RalGAPα2 KO mice, we examined the in vitro and in vivo effects of NLRP3 inhibitors on cell invasion. The number of invading Colon26 cells transfected with RalGAPα2 small interfering RNA (siRNA) decreased significantly after administration of the NLRP3 inhibitor (Figure 8).

Next, we investigated the effect of NLRP3 inhibitor on the AOM/DSS mouse model of the following 4 groups: WT + AOM/DSS, WT + AOM/DSS/NLRP3 inhibitor, RalGAPα2 KO + AOM/DSS, and RalGAPα2 KO + AOM/DSS/NLRP3 inhibitor (Figure 9*A*). Tumor occurrence was examined at the distal end of the colon tissue by endoscopy, macroscopic images, and histopathologic findings, and the representative images of the group of WT + AOM/DSS/NLRP3 inhibitor and RalGAPα2 KO + AOM/DSS/NLRP3 inhibitor are shown in Figure 9*B–D*. The NLRP3 inhibitor did not affect the number of tumors

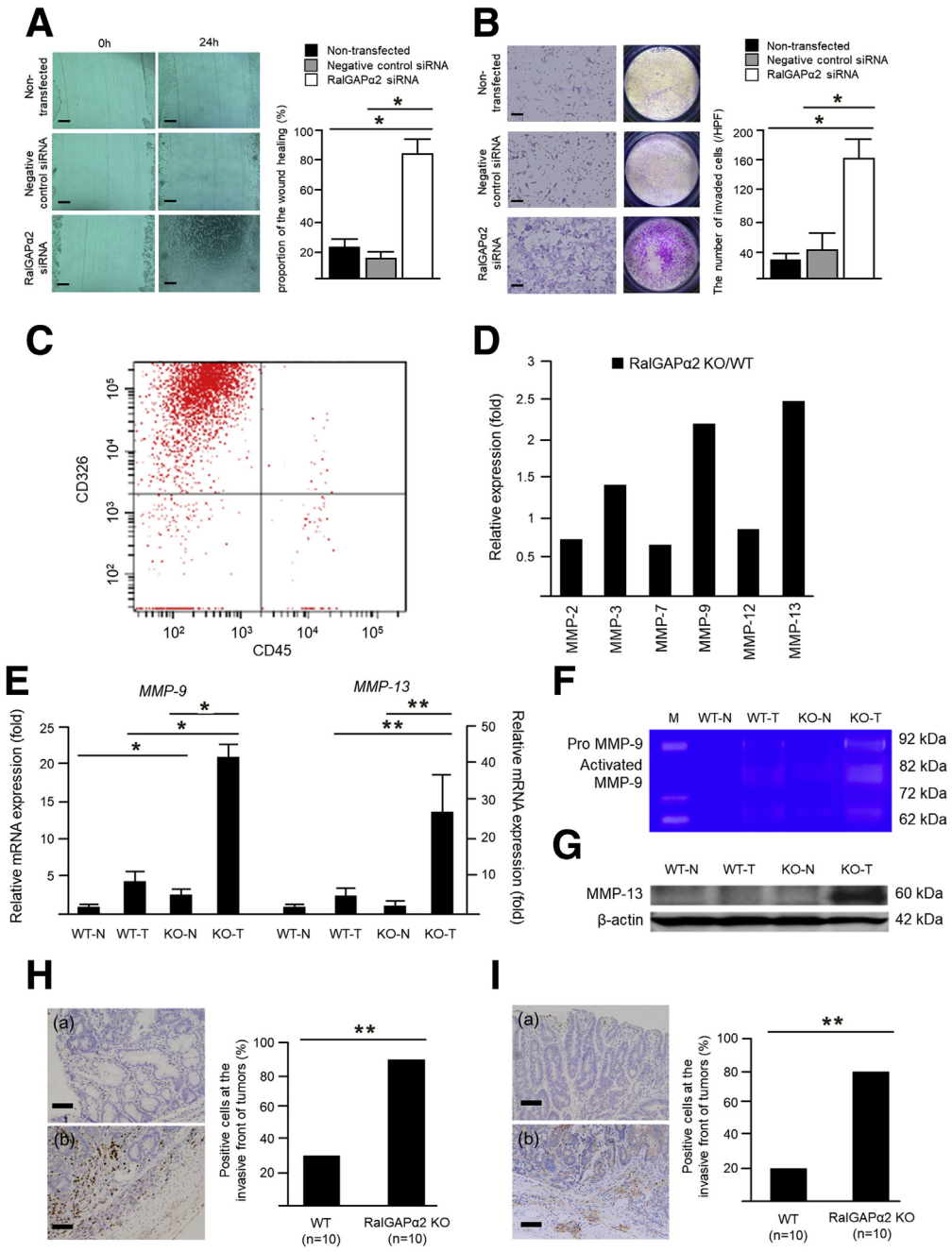

Figure 6. (*A*) In vitro effect of Ral activation on the migration of RalGAPα2 knockdown Colon26 cells. *Scale bars*: 200 μm. *$P < .01$, repeated-measures analysis of variance with the Holm correction. (*B*) In vitro effect of Ral activation on the invasion of RalGAPα2 knockdown Colon26 cells. *Scale bars*: 200 μm. *$P < .01$, 1-way analysis of variance with the Holm correction. (*C*) Flow cytometry findings for the isolated colon epithelial cells that were CD326-positive/CD45-negative. (*D*) The ratio of the gene expression levels of colon epithelial cells in RalGAPα2 KO mice/WT mice. (*E*) The mRNA expression levels of *MMP-9* and *MMP-13* were analyzed by quantitative polymerase chain reaction. The average expression levels in WT-N were defined as 1. *$P < .01$, **$P < .05$, repeated-measures analysis of variance with the Holm correction. (*F*) Gelatin zymography of activated MMP-9 in colon mucosa and CAC. (*G*) Western blot of MMP-13 in colon mucosa and CAC. (*H* and *I*) Immunohistochemical staining for MMP-9 and MMP-13 in the CAC of WT mice (a) and the CAC of RalGAPα2 KO mice (b). *Scale bars*: 100 μm. The proportion of cells that are positive for MMP-9 and MMP-13 at the invasive fronts of tumors from WT mice and RalGAPα2 KO mice (n = 10 per group). **$P < .05$, Fisher exact test. Data are either representative or shown as the means ± SEM (error bars) of 3 independent experiments.

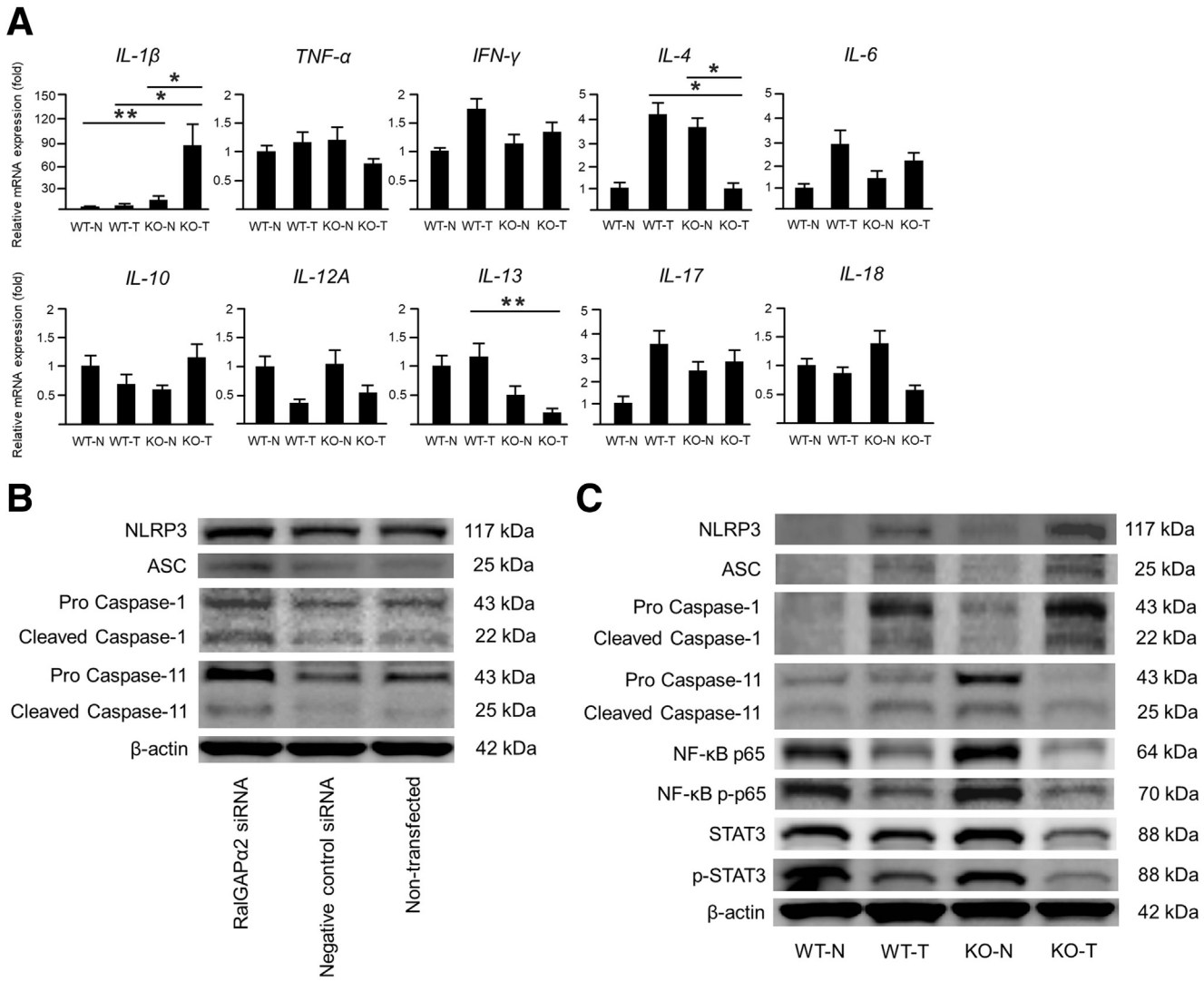

Figure 7. (*A*) The gene expression levels of *IL1β*, *TNF-α*, *IFN-γ*, *IL4*, *IL6*, *IL10*, *IL12A*, *IL13*, *IL17*, and *IL18* were examined in the colon tissues of WT mice and RalGAPα2 KO mice by quantitative polymerase chain reaction. The average expression level in the WT-N was defined as 1. **P* < .01, ***P* < .05, repeated-measures analysis of variance with the Holm correction. (*B*) The differences in the expression levels of NLRP3, ASC, pro/cleaved caspase-1, and pro/cleaved caspase-11 in the controls and RalGAPα2 knockdown Colon26 cells were analyzed by Western blot. (*C*) The differences in the expression levels of NLRP3, ASC, pro/cleaved caspase-1, pro/cleaved caspase-11, NF-κB p65, NF-κB p-p65, STAT3, and phosphorylated STAT3 in colon mucosa and CAC were analyzed by Western blot. Data are either representative or shown as the means ± SEM (error bars) of 3 independent experiments.

in either the AOM/DSS-treated WT group or the RalGAPα2 KO group (Figure 9*E*). However, the mean size of the tumors in the RalGAPα2 KO group treated with NLRP3 inhibitor was decreased significantly in comparison with that in the group without NLRP3 inhibitor treatment (RalGAPα2 KO with NLRP3 inhibitor vs RalGAPα2 KO without NLRP3 inhibitor, 7.0 ± 2.1 vs 5.1 ± 2.0 mm) (Figure 9*F*). With regard to the tendency toward tumor invasion, the ratio of mice with SM invasive tumors in the RalGAPα2 KO group treated with NLRP3 inhibitor was decreased significantly compared with that in the group without NLRP3 inhibitor treatment (RalGAPα2 KO with NLRP3 inhibitor vs RalGAPα2 KO without NLRP3 inhibitor, 45% [9 of 20] vs 10.0% [2 of 20]) (Figure 9*G*). In addition, the number of SM invasive tumors in the RalGAPα2 KO group treated with NLRP3 inhibitor was decreased significantly compared with that in the group without NLRP3 inhibitor treatment (RalGAPα2 KO with NLRP3 inhibitor vs RalGAPα2 KO without NLRP3 inhibitor, 20% [24 of 120] vs 8.8% [6 of 68]) (Figure 9*H*). In addition, the expression of NLRP3, ASC, pro/cleaved caspase-1, MMP-9, and MMP-13 in KO-T were decreased when they were treated with NLRP3 inhibitor (Figure 9*I*–*K*). These results suggest that the Ral-NLRP3 inflammasome pathway with up-regulation of MMPs is involved in the cell invasion phenotype of CAC.

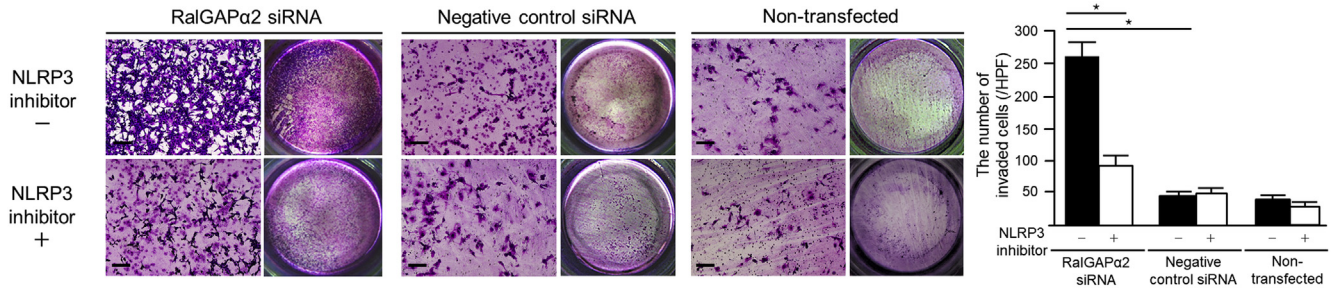

Figure 8. The effect of NLRP3 inhibitor on the invasion of RalGAPα2 knockdown Colon26 cells and the controls. *$P < .01$, 1-way analysis of variance with the Holm correction). Data are either representative or shown as the means ± SEM (error bars) of 3 independent experiments. HPF, high-power field.

RalGAPα2 KD Leads to NLRP3 Transcription via AP-1

The luciferase reporter analysis showed that RalGAPα2 KD Colon26 cells led to mouse NLRP3 transcription when the plasmids did not extend 1.0 kb upstream from exon 1, but when the plasmids extended 1.6 kb (Figure 10*A* and *B*). We focused on some transcriptional factors (Nfatc2, Sox6, AP-1, and Gata1) between this 0.6-kb sequence. The results did not change with the 1.6-kb plasmid except for the sequences of Sox6, Nfatc2, and Gata1. However, the expression of NLRP3 was reduced with the plasmid except for the sequence of AP-1 (Figure 10*C*). These results show that RalGAPα2 KD leads to NLRP3 transcription via AP-1.

Discussion

This study showed a critical role for the down-regulation of RalGAPα2, the major inhibitory regulator of the small GTPase Ral in the colon, in the invasive tumorigenesis of CAC with up-regulation of MMP-9 and MMP-13. In addition, we showed that RalGAPα2 down-regulation induced IL1β expression via NLRP3 inflammasome. Notably, the NLRP3 inhibitor significantly suppressed tumor growth with an invasive phenotype during CAC tumorigenesis, indicating the involvement of decreased RalGAPα2 expression in the progression of CAC via NLRP3 activation with up-regulation of MMPs.

First, we found that RalGAPα2 expression in human CAC decreased significantly compared with that in human sporadic colorectal cancer. Ral activation has been reported to be related to tumor development in some cancers.[11–13] In gastrointestinal cancers, some reports have been found on the association with sporadic colorectal cancer.[14,15] Martin et al[14] reported that activation of RalA is necessary for the anchorage-independent growth of sporadic colorectal cancer. Furthermore, Singhal et al[15] reported that Ral guanine nucleotide exchange factor activation plays an important role as an effector in sporadic colorectal cancer cell lines. Ohta et al[16] reported that the decreased expression of the RasGTPase activating protein is associated with colorectal tumor progression. However, the roles of RalGAP in sporadic colorectal cancer and CAC have not been investigated. In the present study, immunohistochemical analysis indicated that the mechanism of Ral activation in CAC might be different from that in sporadic colorectal cancer. In addition, down-regulation of RalGAPα2 was observed at a more advanced stage in CAC. Therefore, we used RalGAPα2 KO mice with the AOM/DSS model to investigate the role of Ral activation in the development of CAC and compared the histopathologic features of CAC in RalGAPα2 KO mice with those in WT mice. Our data showed that the RalGAPα2 KO mice with the AOM/DSS model showed significantly larger CAC sizes and more invasive phenotypes than the WT mice. We showed significant increases in the RalA/B-GTP and total Ral A/B ratios of CACs in the colon tumor tissue of RalGAPα2 KO mice compared with those in the colon tumor tissues of the WT mice in the AOM/DSS CAC model. Taken together, these data show that Ral activation contributes to the development and invasion mechanism of CAC.

Second, we focused on the contribution of RalGAPα2 on immune cells. WB analysis showed that the expression levels of RalGAPα2 were weak in monocytes, T cells, and B cells (Figure 1*B*). Flow cytometry showed that RalGAPα2 did not influence T-cell or B-cell differentiation or cytokine production of macrophages regardless of the administration of DSS (Figure 2). Furthermore, data on bone marrow chimeric mice showed that RalGAPα2 did not affect immune cell function in the CAC mechanism (Figure 5).

Third, we focused on the mechanism of tumor invasion in RalGAPα2 KO mice. In the AOM/DSS CAC model, colon tumors in RalGAPα2 KO mice showed an invasive phenotype compared with those in WT mice, similar to our previous report with bladder cancer and prostate cancer, which indicated that tumors harboring down-regulated RalGAPα2 were predisposed to tumor invasion.[11,12] However, in those studies, we did not address the molecular mechanism underlying the invasive and metastatic phenotypes.

Here, we attempted to elucidate the mechanism underlying the acquisition of the invasive phenotype in Ral-mediated CACs. First, we performed microarray analysis with colon epithelial cells isolated from both WT and RalGAPα2 KO mice. We found that the gene expression levels of *MMP-9* (gelatinase B) and *MMP-13* (collagenase 3) in the colon epithelial cells of the RalGAPα2 KO mice were more than twice the levels of those in WT mice. Strikingly, we found that the expression levels of MMP-9 and MMP-13 were increased drastically in the CAC tissues of the RalGAPα2 mice. There have been many reports regarding the

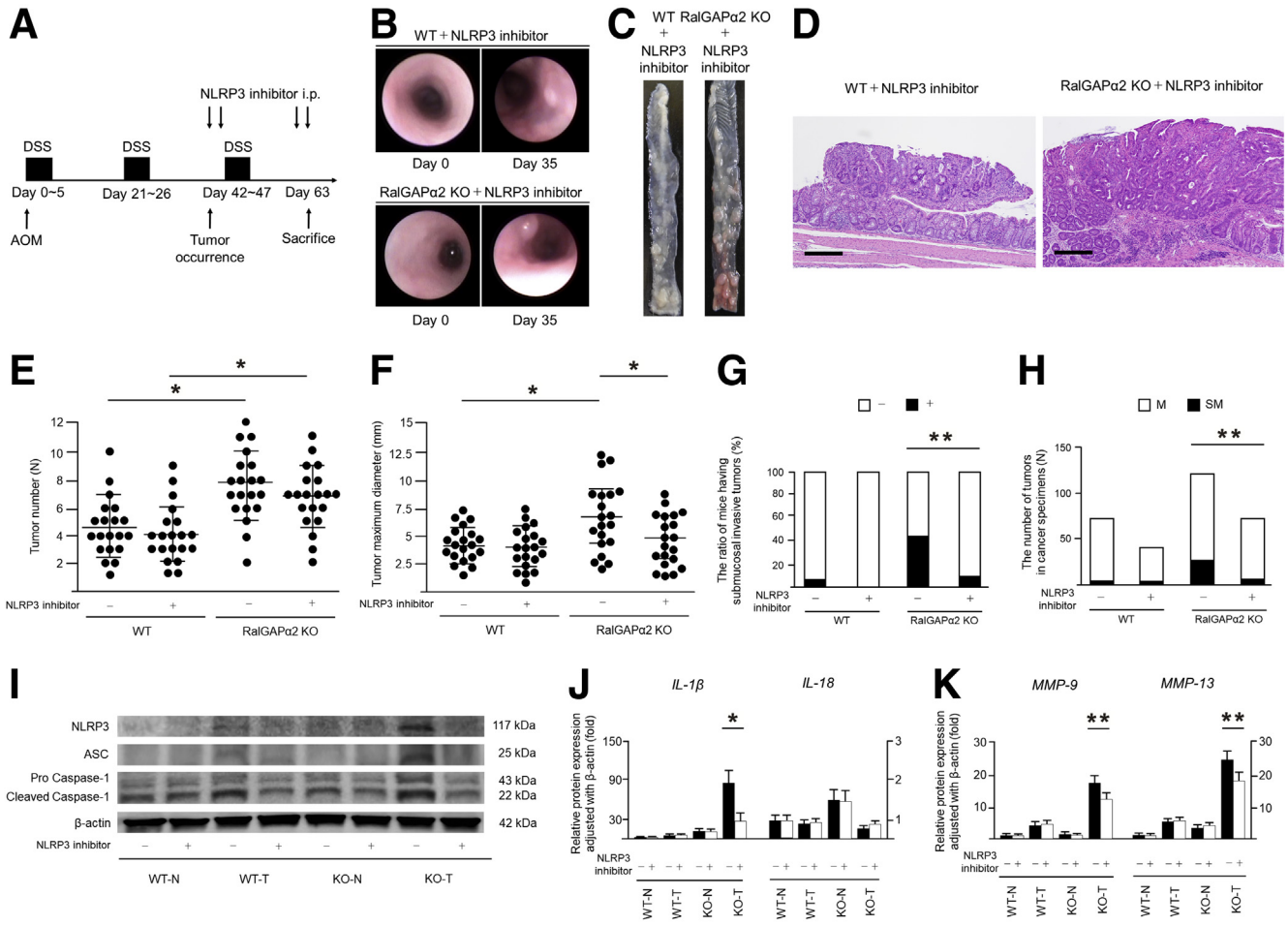

Figure 9. (*A*) The protocol for AOM/DSS/NLRP3 inhibitor administration. (*B*) Endoscopic findings of CAC occurrence with NLRP3 inhibitor administration in WT mice and RalGAPα2 KO mice. (*C*) Macroscopic findings of CAC occurrence with NLRP3 inhibitor administration in WT mice and RalGAPα2 KO mice. (*D*) Histopathologic findings of CAC occurrence with NLRP3 inhibitor administration in WT mice and RalGAPα2 KO mice. (*E–H*) Groups were categorized as follows: WT mice + AOM/DSS, WT mice + AOM/DSS/NLRP3 inhibitor, RalGAPα2 KO mice + AOM/DSS, and RalGAPα2 KO mice + AOM/DSS/NLRP3 inhibitor. (*E–H*) These 4 groups were compared for (*E*) tumor number (*$P < .01$, 1-way analysis of variance with the Holm correction), (*F*) tumor maximum diameter (*$P < .01$, 1-way analysis of variance with the Holm correction), (*G*) the ratio of mice with submucosal invasive tumors (**$P < .05$, Fisher exact test with the Holm correction), and (*H*) the number of submucosal invasive tumors in the cancer specimens (**$P < .05$, Fisher exact test with the Holm correction). M, mucosal tumors. (*I*) The expression of NLRP3, ASC, and pro/cleaved caspase-1 in colon mucosa and CAC with or without NLRP3 inhibitor administration were analyzed by Western blot. (*J* and *K*) The mRNA expression of *IL1β*, *IL18*, *MMP-9*, and *MMP-13* in colon mucosa and CAC with or without NLRP3 inhibitor administration were analyzed by quantitative polymerase chain reaction. Data are either representative or shown as the means ± SEM (error bars) of 3 independent experiments. The average expression level in the WT-N without NLRP3 inhibitor was defined as 1. *$P < .01$, **$P < .05$, repeated-measures analysis of variance with the Holm correction.

critical role of MMPs in cancer invasion and metastasis.[17,18] Our in vitro and in vivo analyses suggested that aberrant Ral activation could contribute to the invasive phenotype of CACs via the induction of MMPs.

Next, we focused on the role of inflammation in CAC. Although various types of cytokines, such as TNF-α, IL1β, IL6, IL10, and IL12/23, are involved in the pathophysiology of IBD,[19] our study yielded the unexpected findings of extremely high IL1β expression in the colon tumors of RalGAPα2 KO mice in comparison with other cytokines, such as Th1, Th2, and Th17 cytokines. Several reports have addressed the association between IL1β and CAC. Neutrophils were found to produce IL1 in experimentally induced colitis and in patients with CAC.[20] Blockade of IL1β activity was shown to reduce tumorigenesis in mice by impairing macrophage-dependent IL6 secretion.[21] Moreover, it was reported that IL1β up-regulates MMP gene expression.[22–24] Taken together, the data in our study indicate that the levels of IL1β produced by cancer cells with down-regulated RalGAPα2 contributed to tumor invasion through MMPs.

When considering IL1β expression in the tumors of RalGAPα2 KO mice, we focused on the association between Ral and the NLRP3 inflammasome. To assess how Ral was involved in NLRP3 inflammasome complex activation, we examined NLRP3 complex activation in Ral-activated colon cancer cell lines and the Ral-activated mouse CAC model.

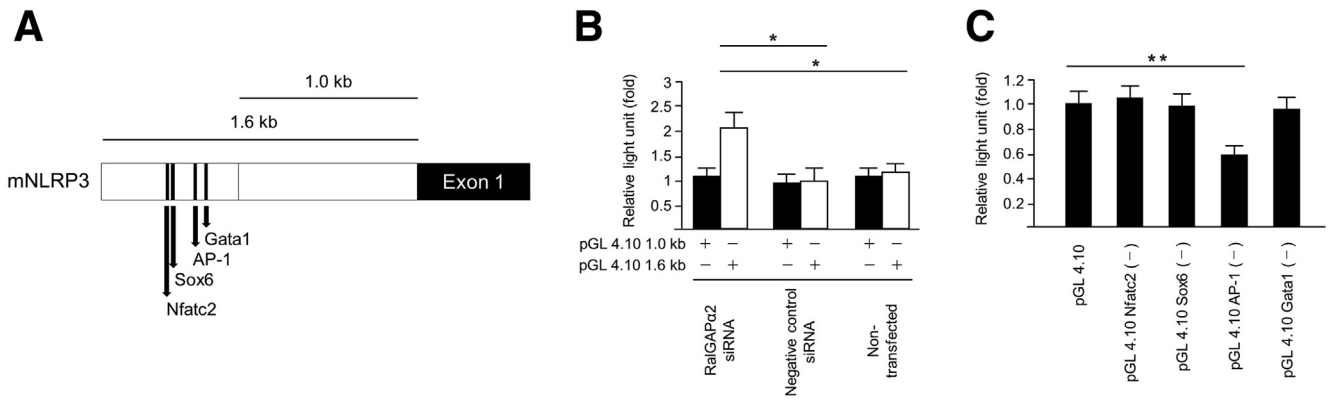

Figure 10. (*A*) The promoter region of mouse NLRP3. (*B*) The expression of NLRP3 was investigated by luciferase reporter assay with pGL 4.10 1.0-kb plasmids or 1.6-kb plasmids on RalGAPα2 knockdown Colon26 cells and controls. *$P < .01$, repeated analysis of variance with the Holm correction. The average expression of Colon26 cells transfected with negative control siRNA and pGL 4.10 1.6-kb plasmids was defined as 1. (*C*) The expression of NLRP3 was investigated by luciferase reporter assay with pGL 4.10 1.6-kb plasmids or pGL 4.10 1.6-kb plasmids without the sequence of Nfatc2, Sox6, AP-1, or Gata1 on RalGAPα2 knockdown Colon26 cells. **$P < .05$, repeated analysis of variance with the Holm correction. The average expression of Colon26 cells transfected with pGL 4.10 1.6-kb plasmids was defined as 1. Data are shown as the means ± SEM (error bars) of 3 independent experiments.

Intriguingly, we found that down-regulation of RalGAPα2 led to NLRP3 inflammasome activation and that NLRP3 inhibition led to decreasing invasive phenotype. However, NLRP3 inhibition did not affect the tumor number but affected its invasive phenotype in vivo. Although a relatively small sample size may have been affected, it was considered that NLRP3 inhibition affected the Ral-NLRP3–MMP pathway and reduced tumor invasion in comparison with tumor enlargement.

Our study showed a significant role for the Ral-activated NLRP3 inflammasome with up-regulation of MMPs in CAC. To date, the role of the inflammasome in CAC progression remains controversial. Several studies have indicated that inflammasome components provide protection against tumorigenesis in CAC.[25,26] In contrast, recent studies have shown that inflammasomes can promote tumor development in CAC.[27,28] In addition, we identified the NLRP3–AP-1 axis under a Ral-activated state. There have been a few reports on the relationship between Ral and AP-1,[29] and between NLRP3 and AP-1.[30,31] However, no reports on the association among Ral, NLRP3, and AP-1 in CAC have been reported. Given our in vitro and in vivo results, the Ral-NLRP3 inflammasome interaction provides new insight into the elucidation of the CAC mechanism.

In this study, IL18 expression in the colon tissues of RalGAPα2 KO mice was not increased in comparison with that in the colon tissues of WT mice, suggesting that RalGAPα2 down-regulation is not involved in IL18 transcription but is deeply involved in IL1β transcription. During the onset or initiation of intestinal inflammation, IL18 plays a protective role.[32] In addition, the administration of exogenous IL18 was reported to alleviate the severity of colitis and colitis-induced tumorigenesis in caspase-1/11 and NLRP3 KO mice.[33] Therefore, a lack of increased IL18 expression might contribute to colitis and colitis-induced tumorigenesis in RalGAPα2 KO mice.

In conclusion, our study showed that RalGAPα2 down-regulation was involved in the mechanism of inflammation-induced colon tumor development. In addition, we identified a possible link between Ral and the NLRP3 inflammasome. Hence, the Ral-NLRP3 pathway can be a potential future therapeutic target for limiting CAC progression.

Materials and Methods

Ethics

This study was performed in accordance with the relevant guidelines and regulations of the animal experiment committee of Sapporo Medical University (Sapporo, Japan). The protocol was approved by the Institutional Committee for Animal Research and the Gene Recombination Experiment Safety Committee at Sapporo Medical University. With regard to human tissues, we used human sporadic colorectal cancer and CAC samples that were obtained surgically at Sapporo Medical University and Hyogo College of Medicine (Nishinomiya, Japan) between 2005 and 2015 under a protocol approved by the institutional review board.

Cell Culture and Chemicals

Human cancer cell lines (lung, A549; breast, MCF7; colon, Colo320; prostate, DU145; and liver, Hep3B), human immune cell lines (monocyte, THP-1; T cell, SupT1; and B cell, Daudi), and a mouse cancer cell line (colon, Colon26) were kindly provided by the laboratory of the National Institutes of Biomedical Innovation, Health and Nutrition, Japanese Collection of Research Bioresources Cell Bank (Osaka, Japan). Cells were maintained in RPMI-1640 medium (cat. R8758; Sigma-Aldrich, St. Louis, MO) containing 10% fetal bovine serum (cat. 26140079; Thermo Fisher Scientific, Waltham, MA) and penicillin plus streptomycin (100 U/mL + 100 μg/mL, respectively).

Table 1. TaqMan Primer-Probe Sets

Gene	Assay ID
MMP-9	Mm00442991_m1
MMP-13	Mm00439491_m1
β-actin	Mm02619580_g1

With regard to RNA interference, we used silencer siRNA targeting mouse RalGAPα2 (cat. 4390771, ID: s109604; Thermo Fisher Scientific). A universal control sequence was used as a negative control (cat. 4390843, silencer negative control no. 1 siRNA; Thermo Fisher Scientific). Colon26 cells were transfected with siRNA at 10 nmol/L using RNAiMAX transfection reagent (cat. 13778075; Thermo Fisher Scientific). Cells were analyzed at 60 hours after transfection.

Murine Care

Male C57BL/6J mice (age, 7 wk) were purchased from Sankyo Labo Service Co (Tokyo, Japan). RalGAPα2 KO mice (C57BL/6J strain) were originally generated as described previously.[11] They were housed in plastic cages (4–6 mice/cage) under controlled conditions of humidity (50% ± 10%), light (12/12-hour light/dark cycle), and temperature (24°C ± 2°C) in specific pathogen-free conditions. Drinking water and a pelleted basal diet were available ad libitum.

Generation of Bone Marrow Chimeric Mice

Cell suspensions from WT or RalGAPα2 KO mice bone marrow were prepared from femurs and tibias, filtered, and counted. Eight- to 12-week-old male WT or RalGAPα2 KO mice received a single intravenous injection of 5.0×10^6 bone marrow cells after total body irradiation using a gamma-ray unit (Gammacell 40; Marubeni Utility Service, Tokyo, Japan). Total body irradiation was administered to recipients in 2 doses (5 Gy + 5 Gy) with a 3-hour interval between the 2 procedures to reduce intestinal damage. Mice then were followed up clinically for 4 weeks. The following groups of chimeric mice were generated: (1) WT to WT, (2) WT to RalGAPα2 KO, (3) RalGAPα2 KO to WT, and (4) RalGAPα2 KO to RalGAPα2 KO mice (Figure 5*A*).

Mouse CAC Model

With regard to the induction of CAC, we injected male mice intraperitoneally (age, 8 wk), and after bone marrow transfusion male mice (ages, 12–16 wk) were given 12 μg/g/body weight AOM (cat. A5486; Sigma-Aldrich) on day 0. Mice were given 2.0% DSS (cat. MFCD00081551, molecular weight 36–50 kilodaltons; MP Biomedicals, Irvine, CA) in water ad libitum for 5 days followed by 16 days of regular drinking water. Then, mice were subjected to an additional 2 DSS cycles.

Furthermore, we intraperitoneally injected glyburide (NLRP3 inhibitor) (cat. NBP2-30141; Novus Biologicals, Littleton, CO) at 50 mg/kg into some male mice daily from tumor occurrence to death according to the AOM/DSS protocol described earlier. The occurrence of CAC was evaluated by endoscopy once a week.

Endoscopic Procedure and Sample Collection

A colonoscopic examination was performed using a microscope system (AVS, Tokyo, Japan), which included a video system (AVS) and a video monitor (Sony, Tokyo, Japan). Mice were anesthetized with isoflurane (cat. 4548995008299; Fujifilm Wako Pure Chemical Cooperation, Osaka, Japan) before endoscopy without preparations, such as fasting or laxatives. Mice were examined endoscopically with respect to inflammation and tumor development in the colon. Colonoscopic examination was performed once a week from day 7 to the end of the study, namely, the 63rd day. Mice were killed on the 63rd day of the experiment.

WT-N, WT-T, KO-N, and KO-T were collected. With regard to histopathologic analysis for colon cancer, the tumor number, tumor maximum diameter, percentage of mice with SM invasion, and percentage of colon cancers with SM invasion among all colon cancers were investigated in our experiments. Tumor number and size were evaluated by visual inspection. In addition, histopathologic examinations of the tumor depth were performed using H&E staining.

Differentiation of T Cells

After the spleen and leg bones were extracted from each mouse at age 8 weeks, the spleen was treated, and CD4+ CD62+ T cells were isolated using a magnetic cell sorting (MACS) system (cat. 130-106-643; Miltenyi Biotec, Bergisch Gladbach, Germany) according to the manufacturer's instructions. These cells were incubated in a 96-well T-cell activation plate (anti-mouse CD3 antibody) (cat. 354720; Corning, Inc, Bedford, MA) for 48 hours, and T-cell differentiation was analyzed by flow cytometry (BD FACSAria II; BD Biosciences, San Jose, CA) using 7-aminoactinomycin D (cat. 420403; BioLegend, San Diego, CA) and a Mouse Th1/Th2/Th17 Phenotyping Kit (cat. 560758; BD Biosciences), including rabbit anti-mouse fluorescein isothiocyanate–interferon-γ, rabbit anti-mouse allophycocyanin–IL4, and rabbit anti-mouse phycoerythrin-IL17A, according to the manufacturer's instructions. These experiments also were performed after 5 days of DSS administration and after 5 days of water drinking.

Differentiation of B Cells

After spleens and leg bones were extracted from each mouse at age 8 weeks, they were treated and CD19+ B cells were isolated using a magnetic cell sorting system (cat. 130-121-301; Miltenyi Biotec) according to the manufacturer's instructions. The differentiation of these cells was investigated by flow cytometry (BD FACSAria II) by using 7-aminoactinomycin D (cat. 420403; BioLegend) and antibodies as follows: rat anti-mouse fluorescein isothiocyanate–IgM (cat. 11-4011-85; Thermo Fisher Scientific) and rat anti-mouse allophycocyanin–IgD (cat. 17-5993-82; Thermo Fisher

Table 2. Primer Sequences

Gene	Forward	Reverse
IL1β	5′-CAACCAACAAGTGATATTCTCCATG-3′	5′-GATCCACACTCTCCAGCTGCA-3′
IL4	5′-CAACCCCCAGCTAGTTGTCA-3′	5′-TGTGGTGTTCTTCGTTGCTG-3′
IL6	5′-TCTGCAAGAGACTTCCATCCA-3′	5′-TCCACGATTTCCCAGAGAACA-3′
IL10	5′-CTATGCTGCCTGCTCTTACTG-3′	5′-AGCAGTATGTTGTCCAGCTG-3′
IL12A	5′-TGAGCTGATGCAGTCTCTGA-3′	5′-CCTTGAGCCTTTCAGGCAGA-3′
IL13	5′-CACTACGGTCTCCAGCCTCC-3′	5′-CCAGGGATGGTCTCTCCTCA-3′
IL17	5′-TCTCTGATGCTGTTGCTGCT-3′	5′-CGTGGAACGGTTGAGGTAGT-3′
IL18	5′-GACAGCCTGTGTTCGAGGAT-3′	5′-GGTCACAGCCAGTCCTCTTA-3′
TNF-α	5′-CATGCACCACCATCAAGGAC-3′	5′-GGCCTGAGATCTTATCCAGCC-3′
IFN-γ	5′-AGCTCTTCCTCATGGCTGTT-3′	5′-ATCTGGCTCTGCAGGATTTT-3′
β-actin	5′-GACCCTGAAGTACCCCATTGAA-3′	5′-AAGGTGTGGTGCCAGATCTTCT-3′

Scientific). These experiments also were performed after 5 days of DSS administration and after 5 days of water drinking.

Cytokines Released From Intraperitoneal Macrophages

Macrophages were collected from both WT and RalGAPα2 KO mice on day 4 after intraperitoneal administration of 5.0% thioglycolate (cat. T0632; Sigma-Aldrich). The macrophages were prepared after removing erythrocytes with red blood cell lysis solution (cat. 158902; Qiagen, Germantown, MD). They were seeded at 1.0×10^6 cells/well in a 6-well culture plate and incubated overnight in medium containing 40 ng/mL recombinant murine macrophage colony-stimulating factor (cat. 315-02; Peprotech, Rocky Hill, NJ). We compared the cytokine levels of the WT mice and RalGAPα2 KO mice by enzyme-linked immunosorbent assay after collecting the culture supernatants of macrophages. These experiments also were performed after 5 days of DSS administration and after 5 days of water drinking.

qPCR, WB, Gelatin Zymography, and Enzyme-Linked Immunosorbent Assay

Total RNA was prepared and reverse-transcribed using a SuperScript VILO complementary DNA Synthesis Kit (cat. 11754050; Thermo Fisher Scientific). The mRNA expression of *MMP-9* and *MMP-13* was analyzed using TaqMan Gene Expression Assays (Thermo Fisher Scientific). Furthermore, the mRNA expression of cytokines derived from mouse colon tissues was analyzed using Power SYBR Green PCR Master Mix (cat. 4367659; Thermo Fisher Scientific). The probes and primer sequences used in this study are shown in Tables 1 and 2, respectively. The gene expression levels of target molecules were normalized to *β-actin* expression.

For the WB analyses, cells and tissues were lysed in RIPA buffer (cat. R0278; Sigma-Aldrich) with protease inhibitor (cat. S8820; Sigma-Aldrich). Protein concentrations were determined with the Bradford method using bovine serum albumin as the standard. The supernatants were boiled in sample buffer (0.05 mol/L Tris-HCl, 2% sodium dodecyl sulfate, 6% β-mercaptoethanol, 10% glycerol, and 1.25% bromophenol blue), subjected to sodium dodecyl sulfate–polyacrylamide gel electrophoresis (10% polyacrylamide gels), and transferred onto polyvinylidene fluoride membranes (cat. SNY0720; Pall Corporation, Pensacola, FL). The membranes were blocked with blocking buffer (Tris-buffered saline with 0.5% Tween-20) containing 5% milk powder and then incubated with primary antibodies overnight at 4°C. Rabbit anti-RalGAPα1-α2 and -β polyclonal antibodies were generated and provided by the author (H.H.). Other primary antibodies that we used were as follows: rabbit anti-RalA (cat. ab96759; Abcam, Cambridge, MA), rabbit anti-RalB (cat. ab129077; Abcam), rabbit anti–MMP-13 (cat. ab39012; Abcam), rabbit anti-NLRP3 (cat. ab214185; Abcam), rabbit anti-ASC (cat. sc-22514-R; Santa Cruz Biotechnology, Dallas, TX), rabbit anti–caspase-1 (cat. ab138483; Abcam), rabbit anti–caspase-11 (cat. ab180673; Abcam), rabbit anti–NF-κB p65 (cat. ab16502; Abcam), rabbit anti–NF-κB p65 (phospho S536) (cat. ab86299; Abcam), rabbit anti-STAT3 (cat. ab68153; Abcam), rabbit anti-STAT3 (phospho S727) (cat. ab30647; Abcam), and mouse anti–β-actin conjugate (cat. 017-24573; Fujifilm Wako Pure Chemical Cooperation). We used horseradish-peroxidase–labeled anti-rabbit IgG as a secondary antibody (cat. 7074P2; Cell Signaling Technology, Inc, Danvers, MA). The membranes were incubated with luminescence detection reagent (cat. 32106; Thermo Fisher Scientific), and we visualized luminescence using an analyzer (LAS-3000; Fujifilm Co, Tokyo, Japan). Densitometric analysis was performed using ImageJ software version 1.52h (National Institutes of Health, Bethesda, MD, available: http://rsbweb.nih.gov/ij/).

In addition, MMP-9 expression was analyzed by gelatin zymography, which was performed using a gelatin zymography kit (cat. PMC-AK47-COS; Cosmo Bio Co, Tokyo, Japan) according to the manufacturer's instructions. The gel was imaged with the detector system (AE-9000 E-graph; ATTO Co, Tokyo, Japan).

An enzyme-linked immunosorbent assay was performed using the IL1β Assay it (cat. MLB00C; R&D Systems,

Minneapolis, MN), IL12A Assay Kit (cat. M1270; R&D Systems), TNF-α Assay Kit (cat. MTA00B; R&D Systems), MMP-9 Assay Kit (cat. MMPT90; R&D Systems), and MMP-13 Assay Kit (cat. CSB-E07413m; Cusabio, Houston, TX), according to the manufacturers' instructions. Sample absorbance was measured at 450/570 nm using a microplate reader (Thermo Fisher Scientific).

Glutathione-S-Transferase–Sec5 Pull-Down Assay

Lysates of Colon26 cells or mouse tissues were centrifuged at 20,900 $\times$ g for 10 minutes. Supernatants containing 200 μg of proteins were incubated at 4°C for 30 minutes with glutathione beads (cat. 17075601, Glutathione Sepharose 4B; GE Healthcare, Uppsala, Sweden) coated with 20 μg of glutathione-S-transferase–Sec5 Ral-binding domain.[4] After washing the beads, the bead-associated GTP-RalA and GTP-RalB were analyzed by WB as described earlier.

Wound Healing Assay

For wound healing assays, Colon26 cells transfected with RalGAPα2 siRNA in 6-well culture dishes were scratched with a plastic pipette tip and cultured for 24 hours. The widths of the wounds (scratched areas) were measured with ImageJ software (http://rsbweb.nih.gov/ij/), and the proportion of wound healing was calculated with the following formula: 100% $-$ (width after 24 hours/width at the beginning) $\times$ 100%. The same procedure also was applied to nontransfected Colon26 cells and Colon26 cells transfected with negative control siRNA.

Cell Invasion Assay

Cell invasion assays were performed using Colon26 cells. In addition, the group was divided into 2 groups according to the presence or absence of 5 μg glyburide (NLRP3 inhibitor) (cat. NBP2-30141; Novus Biologicals) administration. Cell invasion through the Matrigel membrane was quantified using a commercially available cell invasion kit (cat. 354481; Corning, Inc). Colon26 cells (5×10^4 cells/mL) were added to the upper compartments of the chambers and incubated for 22 hours with serum-free RPMI-1640 medium (cat. R8758; Sigma-Aldrich). The cells in the upper chambers were removed, and the cells that had invaded through the Matrigel matrix were stained with May-Giemsa for 2 hours. The extent of infiltration was measured by counting cells.

Microarray Analysis

Phenotypic differences in colonic epithelial cells from both WT mice and RalGAPα2 KO mice were examined. Colonic epithelial cells were isolated from colon tissues, and after flow cytometry using BD FACSAria II (BD Biosciences) was performed to determine whether more than 90% of the isolated cells were CD326-positive/CD45-negative epithelial cells, microarray analysis was performed using a 3D-Gene Human Oligo chip 25k (Toray Industries, Inc, Tokyo, Japan). Microarray slides were scanned using a 3D-Gene Scanner (Toray Industries, Inc) and processed with 3D-Gene Extraction software (Toray Industries, Inc).

Luciferase Reporter Assay

The NLRP3 promoter was inserted into pGL4.10 plasmids containing luciferase sequences (cat. E6651; Promega, Madison, WI) downstream of the promoter, and the plasmids whose concentrations were adjusted to 1 μg/well were transfected into RalGAPα2 KD Colon26 cells using Screen Fect A (cat. 299-73203; Fujifilm Wako Pure Chemical Cooperation). Luciferase activity was measured using the Dual-Luciferase Reporter Assay System (cat. E1910; Promega) with a microplate reader (Infinite M1000 Pro; Tecan, Männedorf, Switzerland), and Renilla luciferase activity was used as the internal control. These experiments were performed with plasmids, except for the Nfatc2, Sox6, AP-1, and Gata1 sequences.

Immunohistochemistry

Immunohistochemistry was performed on 5-μm, formalin-fixed, paraffin-embedded sections. Endogenous peroxidase activity was blocked using 3% hydrogen peroxide, and the sections were incubated overnight at 4°C with primary antibody. The primary antibodies used were as follows: rabbit anti-RalGAPα2, rabbit anti–MMP-9 (cat. ab38898; Abcam), and rabbit anti–MMP-13 (cat. ab39012; Abcam). A subsequent reaction was performed using a horseradish-peroxidase, enzyme-labeled polymer of the Real EnVision detection system (cat. K5007; Agilent, Santa Clara, CA). When a positive reaction was visualized using a diaminobenzidine solution, counterstaining was performed using Mayer's hematoxylin.

For the human samples, normal colon tissues were defined as the distal healthy part with sporadic colorectal cancers. Moreover, CACs were divided into 2 groups: noninvasive (in situ or T1) or invasive (T2-4). The RalGAPα2 expression level of each human sample was graded as strong staining or weak staining. For the mouse samples, the MMP-9 and MMP-13 expression levels of each mouse tissue were graded as strong staining or weak staining at the invasive front of the tumors. These classifications were conducted independently by 2 observers in a blind fashion. Although 80% of the judgments coincided, 20% did not. When the results of the evaluations differed between the 2 observers, the discrepancies were resolved by discussion.

Patient Cohort

We examined patient information regarding age, sex, underlying disease (ulcerative colitis or Crohn's disease), colitis range (left or total), disease duration, and TNM classification in patients with sporadic colorectal cancer or CAC.

Statistical Analysis

To compare groups, categoric variables were compared using the Fisher exact test. Two-group comparisons of mean

values, multigroup comparisons of repeatedly measured samples using ratios relative to the control samples, and multigroup comparisons of repeatedly measured samples using measured values relative to control values were analyzed using the Student t test, repeated-measures analysis of variance, and 1-way analysis of variance, respectively. Multiple comparisons were corrected with the Holm method. A difference was considered significant when $P < .05$. All tests were 2-tailed.

References

1. Terzić J, Grivennikov S, Karin E, Karin M. Inflammation and colon cancer. Gastroenterology 2010;138:2101–2114.e5.
2. Ullman TA, Itzkowitz SH. Intestinal inflammation and cancer. Gastroenterology 2011;140:1807–1816.
3. Chen XW, Leto D, Chiang SH, Wang Q, Saltiel AR. Activation of RalA is required for insulin-stimulated Glut4 trafficking to the plasma membrane via the exocyst and the motor protein Myo1c. Dev Cell 2007;13:391–404.
4. Kawato M, Shirakawa R, Kondo H, Higashi T, Ikeda T, Okawa K, Fukai S, Nureki O, Kita T, Horiuchi H. Regulation of platelet dense granule secretion by the Ral GTPase-exocyst pathway. J Biol Chem 2008; 283:166–174.
5. Henry DO, Moskalenko SA, Kaur KJ, Fu M, Pestell RG, Camonis JH, White MA. Ral GTPases contribute to regulation of cyclin D1 through activation of NF-kappaB. Mol Cell Biol 2000;20:8084–8092.
6. Feig LA. Ral-GTPases: approaching their 15 minutes of fame. Trends Cell Biol 2003;13:419–425.
7. Bodemann BO, White MA. Ral GTPases and cancer: linchpin support of the tumorigenic platform. Nat Rev Cancer 2008;8:133–140.
8. Chien Y, White MA. RAL GTPases are linchpin modulators of human tumour-cell proliferation and survival. EMBO Rep 2003;4:800–806.
9. Shirakawa R, Fukai S, Kawato M, Higashi T, Kondo H, Ikeda T, Nakayama E, Okawa K, Nureki O, Kimura T, Kita T, Horiuchi H. Tuberous sclerosis tumor suppressor complex-like complexes act as GTPase-activating proteins for Ral GTPases. J Biol Chem 2009; 284:21580–21588.
10. Shirakawa R, Horiuchi H. Ral GTPases: crucial mediators of exocytosis and tumourigenesis. J Biochem 2015; 157:285–299.
11. Saito R, Shirakawa R, Nishiyama H, Kobayashi T, Kawato M, Kanno T, Nishizawa K, Matsui Y, Ohbayashi T, Horiguchi M, Nakamura T, Ikeda T, Yamane K, Nakayama E, Nakamura E, Toda Y, Kimura T, Kita T, Ogawa O, Horiuchi H. Downregulation of Ral GTPase-activating protein promotes tumor invasion and metastasis of bladder cancer. Oncogene 2013; 32:894–902.
12. Uegaki M, Kita Y, Shirakawa R, Teramoto Y, Kamiyama Y, Saito R, Yoshikawa T, Sakamoto H, Goto T, Akamatsu S, Yamasaki T, Inoue T, Suzuki A, Horiuchi H, Ogawa O, Kobayashi T. Downregulation of RalGTPase-activating protein promotes invasion of prostatic epithelial cells and progression from intraepithelial neoplasia to cancer during prostate carcinogenesis. Carcinogenesis 2019 May 6. pii: bgz082.
13. Kodama T, Bard-Chapeau EA, Newberg JY, Kodama M, Rangel R, Yoshihara K, Ward JM, Jenkins NA, Copeland NG. Two-step forward genetic screen in mice identifies Ral GTPase-activating proteins as suppressors of hepatocellular carcinoma. Gastroenterology 2016; 151:324–337.e12.
14. Martin TD, Samuel JC, Routh ED, Der CJ, Yeh JJ. Activation and involvement of Ral GTPases in colorectal cancer. Cancer Res 2011;71:206–215.
15. Singhal SS, Singhal J, Yadav S, Dwivedi S, Boor PJ, Awasthi YC, Awasthi S. Regression of lung and colon cancer xenografts by depleting or inhibiting RLIP76 (Ral-binding protein 1). Cancer Res 2007;67:4382–4389.
16. Ohta M, Seto M, Ijichi H, Miyabayashi K, Kudo Y, Mohri D, Asaoka Y, Tada M, Tanaka Y, Ikenoue T, Kanai F, Kawabe T, Omata M. Decreased expression of the RAS-GTPase activating protein RASAL1 is associated with colorectal tumor progression. Gastroenterology 2009;136:206–216.
17. Brown GT, Murray GI. Current mechanistic insights into the roles of matrix metalloproteinases in tumour invasion and metastasis. J Pathol 2015;237:273–281.
18. Shuman Moss LA, Jensen-Taubman S, Stetler-Stevenson WG. Matrix metalloproteinases: changing roles in tumor progression and metastasis. Am J Pathol 2012;181:1895–1899.
19. Neurath MF. Cytokines in inflammatory bowel disease. Nat Rev Immunol 2014;14:329–342.
20. Casini-Raggi V, Kam L, Chong YJ, Fiocchi C, Pizarro TT, Cominelli F. Mucosal imbalance of IL-1 and IL-1 receptor antagonist in inflammatory bowel disease. A novel mechanism of chronic intestinal inflammation. J Immunol 1995;154:2434–2440.
21. Wang Y, Wang K, Han GC, Wang RX, Xiao H, Hou CM, Guo RF, Dou Y, Shen BF, Li Y, Chen GJ. Neutrophil infiltration favors colitis-associated tumorigenesis by activating the interleukin-1 (IL-1)/IL-6 axis. Mucosal Immunol 2014;7:1106–1115.
22. Lim H, Kim HP. Matrix metalloproteinase-13 expression in IL-1β-treated chondrocytes by activation of the p38 MAPK/c-Fos/AP-1 and JAK/STAT pathways. Arch Pharm Res 2011;34:109–117.
23. Tang N, Zhang YP, Ying W, Yao XX. Interleukin-1β upregulates matrix metalloproteinase-13 gene expression via c-Jun N-terminal kinase and p38 MAPK pathways in rat hepatic stellate cells. Mol Med Rep 2013; 8:1861–1865.
24. Gu H, Jiao Y, Yu X, Li X, Wang W, Ding L, Liu L. Resveratrol inhibits the IL-1β-induced expression of MMP-13 and IL-6 in human articular chondrocytes via TLR4/MyD88-dependent and -independent signaling cascades. Int J Mol Med 2017;39:734–740.
25. Allen IC, TeKippe EM, Woodford RM, Uronis JM, Holl EK, Rogers AB, Herfarth HH, Jobin C, Ting JP. The NLRP3 inflammasome functions as a negative regulator of tumorigenesis during colitis-associated cancer. J Exp Med 2010;207:1045–1056.
26. Chen GY, Núñez G. Inflammasomes in intestinal inflammation and cancer. Gastroenterology 2011;141:1986–1999.

27. Guo W, Sun Y, Liu W, Wu X, Guo L, Cai P, Wu X, Wu X, Shen Y, Shu Y, Gu Y, Xu Q. Small molecule-driven mitophagy-mediated NLRP3 inflammasome inhibition is responsible for the prevention of colitis-associated cancer. Autophagy 2014;10:972–985.
28. Zhao Y, Guo Q, Zhao K, Zhou Y, Li W, Pan C, Qiang L, Li Z, Lu N. Small molecule GL-V9 protects against colitis-associated colorectal cancer by limiting NLRP3 inflammasome through autophagy. Oncoimmunology 2017;7:e1375640.
29. Okan E, Drewett V, Shaw PE, Jones P. The small-GTPase RalA activates transcription of the urokinase plasminogen activator receptor (uPAR) gene via an AP1-dependent mechanism. Oncogene 2001;20:1816–1824.
30. Chen XX, Guo Z, Jin Q, Qiao S, Li R, Li X, Deng R, Feng WH, Zhang GP. Porcine reproductive and respiratory syndrome virus induces interleukin-1β through MyD88/ERK/AP-1 and NLRP3 inflammasome in microglia. Vet Microbiol 2018;227:82–89.
31. Jin X, Wang C, Wu W, Liu T, Ji B, Zhou F. Cyanidin-3-glucoside alleviates 4-hydroxyhexenal-induced NLRP3 inflammasome activation via JNK-c-Jun/AP-1 pathway in human retinal pigment epithelial cells. J Immunol Res 2018;2018:5604610.
32. Takagi H, Kanai T, Okazawa A, Kishi Y, Sato T, Takaishi H, Inoue N, Ogata H, Iwao Y, Hoshino K, Takeda K, Akira S, Watanabe M, Ishii H, Hibi T. Contrasting action of IL-12 and IL-18 in the development of dextran sodium sulphate colitis in mice. Scand J Gastroenterol 2003;38:837–844.
33. Zaki MH, Vogel P, Body-Malapel M, Lamkanfi M, Kanneganti TD. IL-18 production downstream of the Nlrp3 inflammasome confers protection against colorectal tumor formation. J Immunol 2010;185:4912–4920.

Received October 23, 2018. Accepted October 3, 2019.

Correspondence
Address correspondence to: Hiroshi Nakase, MD, PhD, Department of Gastroenterology and Hepatology, Sapporo Medical University School of Medicine, Minami 1-jo Nishi 16-Chome, Chuo-ku, Sapporo, Hokkaido, 060-8543, Japan. e-mail: hiropynakase@gmail.com; fax: (81) 11-611-2282.

Acknowledgments
The authors would like to thank Dr Motoya, Dr Igarashi, and the technical staff Hideyuki Koide and Junko Tanba for assistance with experiments. The authors also thank Springer Nature Group (http://authorservices.springernature.com/) for editing a draft of this manuscript.

Author contributions
Tomoya Iida, Daisuke Hirayama, Naoki Minami, and Hiroshi Nakase designed the study; Hiroki Ikeuchi and Seiichi Hirota provided human samples; Ryutaro Shirakawa and Hisanori Horiuchi provided knockout mice; Tomoya Iida, Daisuke Hirayama, Naoki Minami, Minoru Matsuura, Kohei Wagatsuma, Kentaro Kawakami, and Kanna Nagaishi performed the research; Tomoya Iida and Masanori Nojima analyzed the data; Tomoya Iida, Hisanori Horiuchi, and Hiroshi Nakase wrote the manuscript; and Hiroshi Nakase directed the research. All authors helped to perform the research and approved the final draft of the manuscript.

Conflicts of interest
The authors disclose no conflicts.

Funding
This work was supported in part by Health and Labour Sciences Research Grants for research on intractable diseases from the Ministry of Health, Labour and Welfare of Japan (Investigation and Research for Intractable Inflammatory Bowel Disease) (H.N.); the Cooperative Research Project Program of Joint Usage/Research Center at the Institute of Development, Aging and Cancer, Tohoku University (H.H.); and Japan Society for the Promotion of Science Grants-in-Aid for Scientific Research grants JP17J02428 (T.I.), JP18H02799 (H.N.), JP16H05148 (R.S.), and JP16K08574 (H.H.). The funders of the study had no role in the study design, data collection, data analysis, data interpretation, or writing of the report.